RESEARCH ARTICLE

Experimental Study and Thermodynamic Calculations of the Distribution of Ag, Au, Bi, and Zn Between Pb Metal and Pb–Fe–O–Si slag

Denis Shishin[1] · Taufiq Hidayat[2] · Ummul Sultana[1] · Maksym Shevchenko[1] · Evgueni Jak[1]

Abstract

The present article continues the series reviewing the thermochemistry of complex multicomponent pyrometallurgical systems. The recovery of multiple metals through the Pb-based primary and recycling processes is an economic driving force for the circular economy of the future. In this study, equilibrium distributions of Ag, Au, Bi, and Zn between PbO–FeO–Fe$_2$O$_3$–SiO$_2$ silica saturated slag and Pb metal phases were investigated experimentally, using high-temperature equilibration followed by rapid quenching. The measurement of phase compositions was done using microanalytical methods. Electron Probe X-ray Microanalysis (EPMA) was applied for those elements which present at relatively high concentrations. The Laser Ablation Inductively Coupled Plasma Mass Spectrometry (LA-ICP-MS) was used to measure very low concentrations of Ag and Au in slag. The starting mixtures of materials were planned using FactSage software and preliminary thermodynamic database to target specific proportions of phases and concentrations of Pb in slag after the achievement of equilibrium. Measured slag/metal distribution coefficients follow the sequence Zn ≫ Ag > Bi ≫ Au. Newly obtained results were critically assessed and used to improve the thermodynamic database. Integration between experiments and thermodynamic database development permits cross-analysis of distribution coefficients obtained in the present study with the parallel measurements of distribution in copper-based systems. The liquid slag phase was described using a two-sublattice Modified Quasichemical Model (MQM). Single sublattice MQM was applied for the liquid metal phase.

Keywords Recycling · Phase equilibrium · Lead smelting · EPMA · FactSage · Distribution coefficient · Minor elements · Gold recovery · Silver recovery

Introduction

The circular economy of the future will rely on sustainable metallurgy. Efficient recovery of several valuable metals in the same process is necessary to provide the economic incentive for changes in the industry. Minor elements can be extracted using either pyrometallurgical or hydrometallurgical processing routes [1]. Presently, successful recyclers such as Umicore (Belgium) and Boliden (Sweden) use the integrated pyrometallurgical and hydrometallurgical processing [2] of primary and secondary copper/lead materials. The development of complex and flexible flowsheets requires a solid thermodynamic foundation for predictions of phase equilibria, distribution of elements, and heat balances. Large multicomponent thermodynamic databases provide the necessary predictions. The accuracy of predictions is higher if they rely on the experimental results [3, 4]. A combination of thermodynamic modeling and experimental measurements of minor elements in the copper-based Cu–Fe–O–S–Si system has recently been reported for Sb, Sn [5], As [6], Ag, and Au [7]. The Pb–Fe–O–Si system forms the foundation for the lead-based processes. No systematic study of phase equilibria in this system was available until recent works by Shevchenko and Jak [8–10]. The only data available for the compositional range of the liquid slag phase close to lead smelting conditions belong to the Ca–Pb–Fe–O–Si system

✉ Denis Shishin
d.shishin@uq.edu.au

1   PYROSEARCH, School of Chemical Engineering, University of Queensland, Brisbane, QLD 4072, Australia

2   Metallurgical Engineering Department, Faculty of Mining and Petroleum Engineering, Institut Teknologi Bandung, West Java 40132, Indonesia

[11]. Similarly, no measurements of the distribution coefficients of minor elements between PbO–FeO–Fe$_2$O$_3$–SiO$_2$ slag and Pb metal are available in the literature. The only study found in literature is for the distribution coefficient of Ag between PbO–FeO–Fe$_2$O$_3$–CaO–SiO$_2$ slag and metallic lead [12]. In the present study, the first experimental results for Ag, Au, Bi, and Zn distributions in the Pb–Fe–O–Si system are reported, analyzed thermodynamically, and compared with the earlier results in the Ca–Pb–Fe–O–Si system [12].

Research Methodology

Integration of Experiments and Thermodynamic Database Development

In the present study, experiments and thermodynamic modeling were performed in parallel. An integration of studies in several systems, such as copper smelting and lead smelting, increases confidence in the results. At first, a thermodynamic database was developed based on existing phase diagram, activity, distribution, and calorimetric data. It was then used to identify gaps in the experimental knowledge, to suggest the conditions of experiments, and to analyze the results. New experiments are used to improve the thermodynamic database, maintaining agreement with the complete experimental dataset. A detailed description of the database development process and examples of the integrated experimental and thermodynamic modeling approach was given by Jak [13].

Experimental Technique

The experimental methodology involves high-temperature equilibration, rapid quenching, and direct measurement of the compositions of the condensed equilibrated phases using microanalysis techniques [13, 14]. To confirm that the chemical system reached equilibrium conditions, the four-point test is applied, namely: effect of the equilibration time, phase homogeneity, approaching equilibrium from the opposite directions, and kinetic study of the reactions possible inside the selected system. These effects were systematically analyzed in the earlier study of equilibrium between Pb metal and Pb–Fe–O–Si slag without minor elements [9]. Based on many trials, the use of master slags and equilibration time of 1–3 h were recommended for temperatures 1373–1573 K [1100–1300 °C]. Longer heating resulted in high chance of ampoule failure.

As a measure to prevent the evaporation of lead oxide and increase the speed of reaction, two master slags were prepared. The PbO–SiO$_2$ master slag was prepared from PbO (99.9 wt% purity) and SiO$_2$ (99.9 wt% purity) with the composition of 60 mol% SiO$_2$. The fayalite master slag, close to the composition of Fe$_2$SiO$_4$, was prepared from Fe powder (99.998 wt%), Fe$_2$O$_3$ (99.945 wt%), and SiO$_2$ (99.9 wt% purity) as described earlier [9, 15]. Master slags were then crushed and mixed with extra silica, PbO, ZnO (99.8 wt% purity), Bi$_2$O$_3$ (99.9 wt%), Ag (99.9 wt%), Au (99.5 wt%), and Pb powder (99.95 wt% purity). The weights were calculated in FactSage [16] to produce 0.25 grams of slag, 0.25 grams of metal, and 0.01 grams of tridymite in each sample after the equilibration. High-temperature equilibration of premixed metals and oxides was performed on a SiO$_2$ substrate of high purity inside a vertical tube furnace at temperatures between 1273 and 1473 K [1000 and 1200 °C] under pure argon gas atmosphere. The sealed silica ampoule, Fig. 1a, prevents the vaporization of Pb and volatile minor elements. After 3 h of heating time, samples were quenched at a very high rate, hundreds degrees per second, then mounted in epoxy resin. Cross-cuts were polished for microanalysis. The concentrations of major components in the phases were measured by an electron probe X-ray microanalyzer (EPMA), JEOL JXA 8200L (trademark of Japan Electron Optics Ltd., Tokyo). An acceleration voltage of 15 keV and a probe current of 15 nA were used. Results were corrected by the Duncumb–Philibert ZAF correction procedure supplied with the JEOL JXA 8200L probe. Appropriate reference materials from Charles M. Taylor, Stanford, CA (SiO$_2$, Fe$_2$O$_3$, Bi, Ag, Au), NIST K456 PbO–SiO$_2$ glass, and sintered pure ZnO powder were used as standards. Additional correction was then applied to slag composition according to [8, 9]. The average compositions of the slag and metal phases were determined using the EPMA line analysis approach with beam diameters between 10 and 50 μm. As discussed in the work by Fallah-Mehrjardi et al. [17], the increase of the probe diameter reduces the uncertainty in the composition measurement.
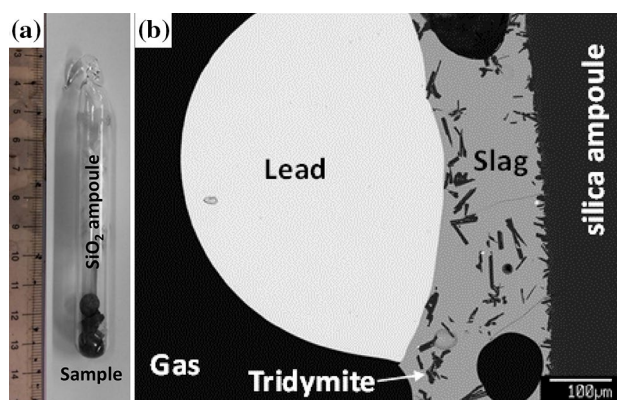

Fig. 1 a Sealed silica ampoule with sample inside before the equilibration, **b** Microstructure of quenched sample showing slag/Pb metal/tridymite equilibria in the Pb–Fe–O–Si system containing Ag, Au, Bi, and Zn at 1473 K [1200 °C]

Laser Ablation Inductively Coupled Plasma Mass Spectrometry (LA-ICP-MS) was used to measure the concentrations of Ag and Au in the slag. The NWR193 Laser Ablation System (Electro Scientific Industries Inc, Portland, USA) and an Agilent 8800 ICP-MS (Agilent Technologies, Santa Clara, USA) were used. Two certified synthetic glass reference materials NIST610 (containing 380 ppm Bi, 239 ppm Ag, and 23 ppm Au) and NIST612 (containing 30 ppm Bi, 22 ppm Ag, and 5 ppm Au) were used as standards. An ablation diameter between 30 and 65 μm for the slag phase was used to obtain representative compositions.

The procedures for improving the detection limit, reproducibility, and accuracy of the LA-ICP-MS measurements have been described in detail by Chen et al. [18]. For the slag phase, estimated detection limit with EPMA is about 200 ppm or 0.02 wt% for Bi, Ag, and Au. Detection limit of 0.01 wt% is estimated for Zn in metal. Using the LA-ICP-MS technique allows detecting 0.02 ppm of Bi, Ag, and Au in slag. The technique to measure elements in metal using LA-ICP-MS is not yet developed due to the problems with consistent ablation of low-melting phases. The precision of LA-ICP-MS from 5 repeated measurements of NIST 612 glass standard was within 1–2% of the measured value. The accuracy was determined by measuring NIST 610 glass as unknown and using NIST 612 as a standard for Bi and Ag. The accuracy of 3% for Bi, 9% for Ag, and 4% for Au was obtained.

Thermodynamic Modeling

The FactSage 7.3 thermodynamic package [16] and a private thermodynamic database developed in PYROSEARCH were used for calculations in the present study. Table 1 lists the thermodynamic models for slag, liquid metal, spinel, and tridymite.

The spinel model, developed using the Compound Energy Formalism [21], was described in the assessments of the Fe–Zn–O [25] and Fe–O [24] systems. Tridymite stoichiometric compound was taken from the study of Eriksson and Pelton [23]. Mathematical expressions for the Modified Quasichemical Model can be found in the publications by Pelton

et al. [19, 20]. Critical assessment and model parameters for the relevant slag systems are available in earlier publications: Fe–O [26], Fe–O–Si [27], Pb–O–Si [28], Pb–Fe–O [10, 29], and Pb–Fe–O–Si [10, 29].

Model parameters for the metal phase were taken from thermodynamic assessments available in the literature: Pb–Ag [30], Pb–Au [31], Pb–Zn [32], and Pb–Bi [33]. The random mixing Bragg–Williams model with Redlich–Kister expansion of excess parameters [22] was used in all of these studies.

The introduction of the minor elements in the slag solution requires knowledge of their oxidation states. Based on recent experimental and modeling studies [7, 34], 1+ oxidation state is assigned to Ag and Au. The 2+ oxidation state for Zn is widely accepted and successfully used in the earlier thermodynamic models [25, 28, 29]. Some controversy existed for the oxidation state of Bi in slag as Nagamori et al. [35] and Chen and Wright [36] have reported the oxidation states of 0, and 2+ respectively. Recent better controlled measurements by Hidayat et al. [34] clearly indicated only Bi^{3+} in slag. This is also in agreement with other authors [37, 38] and accepted in the present study.

Once the oxidation state of an element in the slag solution is selected, the Gibbs energy of the corresponding end-member must be assigned. Gibbs energies of oxides of minor elements in slag have the largest effect on the distribution coefficients. The secondary effect of slag composition on the distribution coefficient is introduced by the excess parameters: MO_x–SiO_2, MO_x–PbO, MO_x–PbO–SiO_2, MO_x–FeO, MO_x–Fe_2O_3, MO_x–FeO–SiO_2, and MO_x–Fe_2O_3–SiO_2, where MO_x stands for minor element oxide. The present study is conducted in close integration with the experimental and modeling investigations of the copper-based systems, so that the selected thermodynamic properties of minor elements in slag must describe the existing data for the distribution coefficient slag/Pb metal, as well as data for slag/copper metal and slag/Cu_2S–FeS matte.

Thermodynamic properties of Ag_2O component of slag were reproduced using the assessment of Assal et al. [39]. The distribution coefficient of silver between fayalite slag and copper, as reported by Shishin et al. [7] and unpublished

Table 1 List of phases and thermodynamic models of the present study

Phase name	Model	Short notation used in this study
Tridymite	Stoichiometric [23]	SiO_2
Spinel (Magnetite)	$(Fe^{2+}, Fe^{3+}, Zn^{2+})^{tetr}[Fe^{2+}, Fe^{3+}, Zn^{2+}, Va]_2^{oct}O_4^{2-}$, CEF [24]	Spinel
Liquid oxide (Slag)	$(Pb^{2+}, Fe^{2+}, Fe^{3+}, Si^{4+}, Ag^+, Au^+, Bi^{3+}, Zn^{2+})(O^{2-})$, MQM	Slag
Liquid metal	(Pb, Fe, O, Ag, Au, Bi, Zn), B-W + R-K	Pb (liq)

MQM modified quasichemical model [19, 20], *CEF* compound energy formalism [21], B-W + R-K = Bragg–Williams ideal mixing model plus Redlich–Kister expansion of excess parameters [22]

data by Shevchenko and Shishin [40] for high PbO-slags in equilibrium with silver were used to optimize a set of model parameters, Ag_2O–SiO_2, Ag_2O–PbO, Ag_2O–FeO, Ag_2O–Fe_2O_3, and Ag_2O–PbO–SiO_2. These parameters were used in the present study for thermodynamic calculations.

The thermodynamic database for Au_2O was created to best describe the dataset of the following studies. Borisov and Palme [41] investigated an equilibrium between Al_2O_3–CaO–MgO–SiO_2 slag and Pd-Au alloy at 1300–1430 °C and $P(O_2) = 10^{-11.5}$ to 1 atm. Han et al. [42] equilibrated Al_2O_3–CaO–MgO–SiO_2 slag with gold metal at 1350–1500 °C and $P(O_2) = 10^{-9.5}$–10^{-8} atm. Swinbourne et al. [43] studied PbO slag in equilibrium with gold metal at 1100 °C and $P(O_2) = 10^{-3}$, 0.21, and 1 atm; PbO–SiO_2 slags in equilibrium with gold at 1100 °C and $P(O_2) = 0.21$ atm; FeO–Fe_2O_3–SiO_2 slags in equilibrium with gold at 1300 °C and $P(O_2) = 10^{-9}$–10^{-7} atm; CaO–FeO–Fe_2O_3 slag in equilibrium with gold at 1300 °C and $P(O_2) = 10^{-1}$–10^{-7} atm. Avarmaa et al. [44] measured the distribution of gold between Al_2O_3–Cu_2O–FeO–Fe_2O_3–SiO_2 slag and metallic copper at 1300 °C and $P(O_2) = 10^{-10}$–10^{-5} atm. Sukhomlinov et al [45] measured the distribution of gold between Cu_2O–FeO–Fe_2O_3–SiO_2 slag and metallic copper at 1300 °C and $P(O_2) = 10^{-7}$–10^{-4} atm. Shishin et al. [7] measured the equilibrium with FeO–Fe_2O_3–SiO_2 slag and gold at 1250 °C and $P(O_2) = 10^{-8}$–$10^{-6.5}$ atm; as well as the distribution of gold between FeO–Fe_2O_3–SiO_2 slag and Cu_2S–FeS matte at 1200 °C, $P(SO_2) = 0.25$ atm. Avarmaa et al. measured the distribution of gold between FeO–Fe_2O_3–SiO_2 slag and Cu_2S–FeS matte at 1250–1350 °C and $P(SO_2) = 0.1$ atm. All the solubility data were recalculated to ppm Au in slag divided by activity of Au. Analysis showed that the results of Borisov and Palme [41], and slag/gold of Shishin et al. [7] were on average ten times lower in terms of ppm(Au in slag)/a(Au), compared to other studies. These were excluded from the experimental dataset. The Gibbs energy of Au_2O in slag and the excess parameters were introduced to optimize all the remaining data. Model parameters Au_2O–SiO_2, Au_2O–PbO, Au_2O–FeO, Au_2O–Fe_2O_3, and Au_2O–PbO–SiO_2 are relevant to the present study and were used in the thermodynamic calculations. The details of the optimization procedure will be reported elsewhere.

Gibbs energy of liquid ZnO is taken from Jak et al. [46]. The experimental phase diagrams obtained for the ZnO–SiO_2 [28], PbO–ZnO, and PbO–ZnO–SiO_2 systems [15], as well as the Zn–Fe–Si–O system [47, 48], were optimized by Shevchenko [29]. The resulting excess parameters were used in the present study.

For Bi_2O_3, the thermodynamic assessment of Risold et al. [49] was used to fix the Gibbs energy of Bi_2O_3 in slag. Activity and phase diagram data in the Bi_2O_3–PbO and Bi_2O_3–SiO_2 systems were reported by Diop [50] and Onderka [51], respectively. Model parameters in the slag

solution were optimized to reproduce the results of these authors. For the Bi_2O_3–Fe_2O_3 system, a tentative phase diagram is available from Lu et al. [52] and Maitre et al. [53]. The Bi_2O_3–Fe_2O_3 parameters in slag were introduced and optimized to describe best the hematite and Bi_2O_3 liquidi, but discrepancies were identified between studies of the enthalpy of formation of solid phases, $BiFeO_3$ and $Bi_2Fe_4O_9$ [54], so the liquidus for these phases as proposed by Lu et al. [52] could not be reproduced. The Bi_2O_3–FeO parameter is adjusted to describe distribution data between slag and copper by Hidayat et al. [34].

Results

High-Temperature Equilibration Experiments

Figure 1b shows a typical microstructure of the slag/Pb metal/tridymite equilibrium phases. Plate-like tridymite crystals were observed in the slag with thickness approximately 5 to 10 μm. Slag phase is in contact with the silica tube wall, while the lead metal droplet is "sitting on top" of the slag. The position of metal droplet is controlled by the surface tension, in contrast to large samples, where the position of metal is at the bottom of the crucible due to higher density. Slag composition was analyzed in the areas free from tridymite. Table 2 gives the compositions of phases in equilibrium. The ratios of the different oxidation states of iron cations cannot be measured using the EPMA, and the iron oxide concentrations were recalculated as FeO for presentation purposes. The proportion $Fe^{3+}/(Fe^{3+} + Fe^{2+})$ increases with increasing wt% Pb in slag due to higher $P(O_2)$ in the system. This fact is taken into account in the thermodynamic calculations. Ag, Au, and Bi predominantly partition to the Pb metal phase, while Zn preferably partitions to the slag phase as ZnO. The concentration of Zn in the metal phase was very low, about 0.01–0.03 wt%, which is close to the detection limit of EPMA. Under these conditions, lower relative accuracy of measurement can be achieved. In the slag phase, the concentration of Au was less than 0.05 ppm, which is close to the detection limit of LA-ICP-MS.

The measured composition of the slag in terms of major elements and the distribution coefficients of minor elements are shown in Figs. 2 and 3. The distribution coefficient is expressed as the slag/metal concentration ratio. The results show a decrease in the distribution coefficient in the sequence Zn ≫ Ag > Bi ≫ Au. In practice, this means that zinc will partition almost completely to the slag phase, while gold will concentrate mostly in the metallic Pb. The main losses of gold in slag would be due to the physical entrainment of metal particles in the slag.
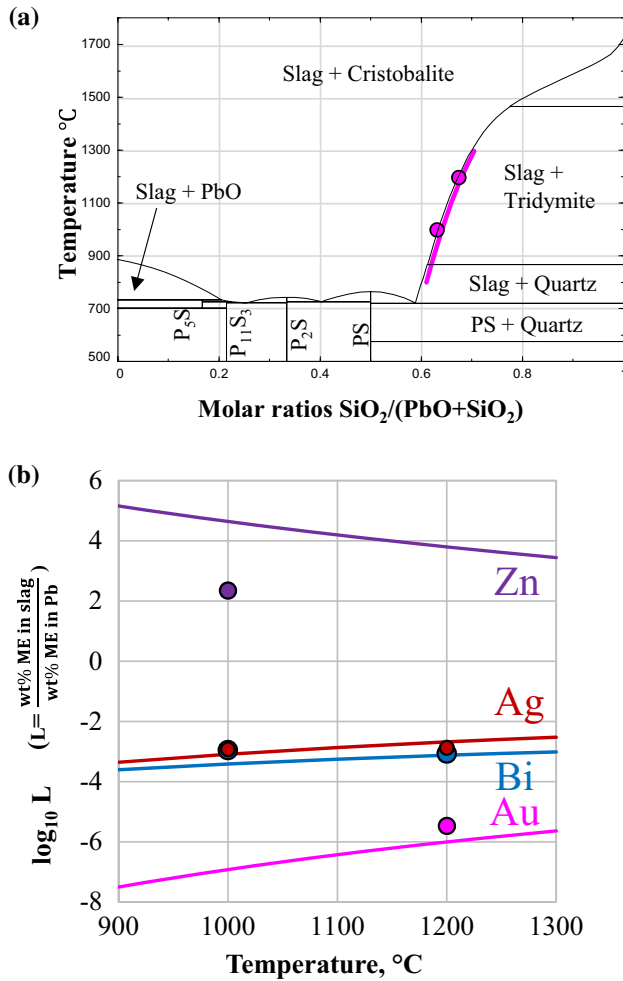
Table 2 Measured phase compositions for the slag/Pb metal/tridymite equilibria in the Pb–Fe–O–Si system containing Ag, Au, Bi, and Zn minor elements

No	Temp, K [°C]	Phase	Metal/Oxide (wt pct)			Old Total[a]	Pb in slag	ME unit	Minor elements				$\mathrm{Log}_{10}\left[L_{Ag}^{sl/Pb}\right]$	$\mathrm{Log}_{10}\left[L_{Au}^{sl/Pb}\right]$	$\mathrm{Log}_{10}\left[L_{Bi}^{sl/Pb}\right]$	$\mathrm{Log}_{10}\left[L_{Zn}^{sl/Pb}\right]$
			Pb / PbO	Fe / FeO	Si / SiO₂				Ag	Au	Bi	Zn				
1	1273 [1000]	Metal	99.9	0.08	0.00	N/A		wt pct	1.34	0.33	1.12	0.01	N/A	N/A	N/A	
		Slag	68.4	0.01	31.55	N/A	62.4	ppm	N/A	N/A	N/A	22,959				2.36
2	1273 [1000]	Metal	100.0	0.02	0.01	95.03		wt pct	1.71	0.46	1.66	0.01	−2.92	N/A	−2.95	
		Slag	68.5	0.01	31.4	101.37	62.6	ppm	20.4	N/A	18.5	20,125				2.30
3	1473 [1200]	Metal	100.0	0.02	0.01	96.50		wt pct	1.58	0.32	1.13	BDL	−2.88	−5.51	−3.07	
		Slag	64.3	0.00	35.67	101.84	58.6	ppm	20.9	0.01	9.7	20,579				N/A
4	1473 [1200]	Metal	99.9	0.07	0.05	94.64		wt pct	5.9	2.4	1.13	BDL	−3.10	−5.90	−3.30	
		Slag	47.6	17.63	34.7	101.86	43.6	ppm	47.2	0.03	5.7	16,674				N/A
5	1473 [1200]	Metal	100.0	0.02	0.00	N/A		wt pct	2.2	0.80	1.15	0.03	N/A	N/A	N/A	
		Slag	45.1	20.1	34.8	N/A	41.4	ppm	N/A	N/A	N/A	17,428				1.76
6	1473 [1200]	Metal	99.9	0.07	0.01	95.97		wt pct	1.97	0.60	1.66	0.03	−2.64	−5.08	−3.69	
		Slag	29.8	35.7	34.4	102.35	27.4	ppm	45.3	0.05	3.4	14,623				1.69
7	1473 [1200]	Metal	100.0	0.04	0.00	95.39		wt pct	2.2	1.00	2.0	0.01	−2.69	−5.30	−3.77	
		Slag	14.7	49.3	35.8	101.26	13.5	ppm	45.3	0.05	3.4	12,682				2.10

N/A not available, *BDL* below detection limit

[a]Old total is the sum of concentrations originally calculated by EPMA software based on standards and ZAF corrections. Compositions in Table are normalized to 100% total

Fig. 2 **a** Phase diagram of the PbO–SiO$_2$ system [28]. Symbols (circle) show the projection of slag composition measured in the present study, points No 1–3. Thick purple line is the calculation corresponding to experimental conditions of the present study. **b** Distribution coefficients of Ag, Au, Bi, and Zn between slag and liquid Pb, points No 1–3. Symbols (circle) show experimental results of the present study, lines are thermodynamic calculations (Color figure online)

Fig. 3 **a** Phase diagram of the Pb–Fe–O–Si system in equilibrium with Pb metal. Slag composition is projected onto the FeO–PbO–SiO$_2$ plane through the oxygen corner [29]. Symbols (circle) show the projection of slag composition measured in the present study, points No 3–7. Thick magenta line is the calculation corresponding to experimental conditions of the present study. **b** Distribution coefficients of Ag, Au, Bi, and Zn between slag and liquid Pb at 1200 °C. Symbols (circles) show experimental results of the present study, points No 3–7, lines are thermodynamic calculations. Thick magenta line (modeling result) and symbols (circles) (experimental results) present the effects of Zn addition on liquidus line at 1473 K [1200 °C] (Color figure online)

Thermodynamic Calculations and Analysis of the Results

Thermodynamic calculations were performed using the Equilib module of FactSage 7.3 software [16]. The amounts of input components, FeO, PbO, SiO$_2$, and Pb were selected to obtain the equilibrium between slag, liquid Pb, and a solid phase: tridymite, Fe metal, wüstite, or spinel. Projected slag composition is shown using the thick purple line in Figs. 2a and 3a. In the calculation, PbO acts as a source of oxygen and converts some of FeO into Fe$_2$O$_3$ and minor elements into oxides. The average concentrations of elements in the metal phase according to Table 2 are 2.4 wt% Ag, 0.8 wt% Au, and 1.4 wt% Bi. The average concentration of Zn in slag is 1.8 wt%. In the calcul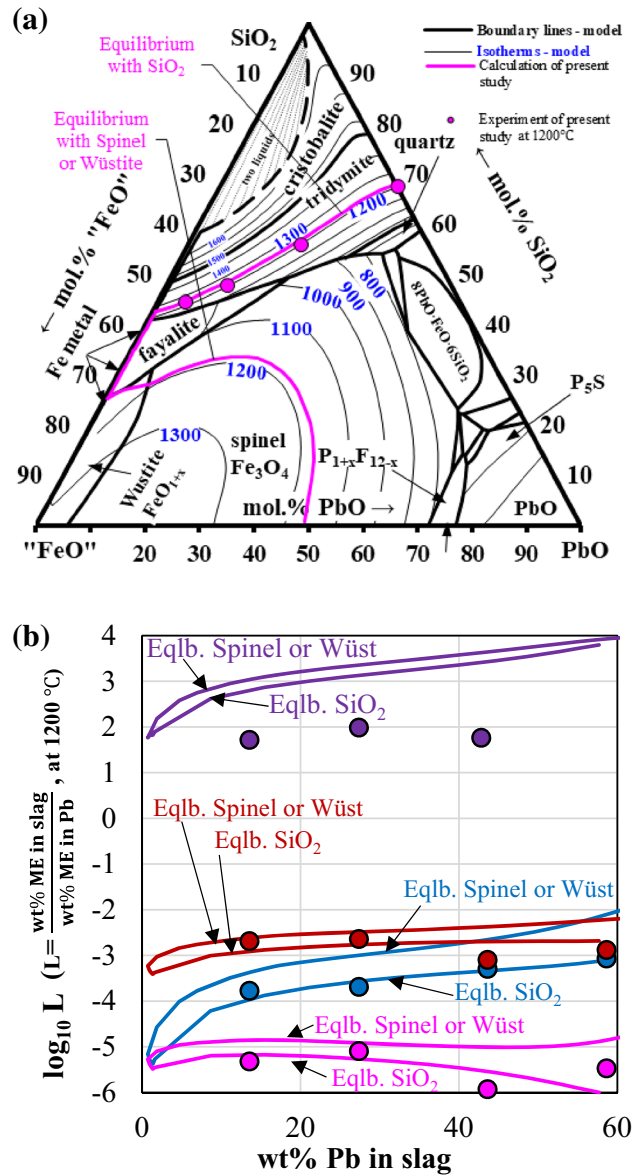ation, the amounts of Ag, Au, Bi, and Zn were added and adjusted iteratively to achieve the fixed target concentrations of 2.4 wt% Ag in metal, 0.8 wt% Au in metal, 1.4 wt% Bi in metal, and 1.8 wt% Zn in slag. As demonstrated by Yazawa [55], the distribution coefficient of minor elements between slag and metal depends on the

oxygen partial pressure and ratio of activity coefficients in metal and slag. At fixed $P(O_2)$, and within a narrow range of concentration of a minor element, the distribution coefficient is practically independent of concentration because the ratio of activity coefficients is constant. Calculations were performed for several concentrations of minor elements and confirmed that the distribution coefficients practically did not change. In Fig. 3b, every calculated distribution line "loops" through the primary precipitation phase fields of tridymite, Fe metal, olivine, wüstite, and spinel. It shows the effect of (Fe + Pb)/SiO$_2$ ratio in slag on the distribution coefficient, as predicted by the model. The calculated sequence of distribution coefficients is consistent with the experiments: Zn ≫ Ag > Bi ≫ Au. The calculated distribution coefficient for Zn is higher than the experimental values. For the fixed concentration of Zn in slag, this means lower calculated concentration in the metal phase, than measured. For Au, the calculated distribution coefficient is lower than in the experiment. For the fixed concentration of Au in the metal phase, this means lower calculated concentration in the slag, compared to the measured values.

Figure 3a demonstrates the effects of ZnO in slag on the 1473 K [1200 °C] tridymite liquidus comparing to the calculations of Shevchenko [10] in the Pb–Fe–O–Si system. According to the thermodynamic model, the presence of ZnO in the slag results in the small shift of the tridymite liquidus to lower (Fe + Pb)/SiO$_2$. In other words, small amount of ZnO in slag decreases the tridymite liquidus. The effect is very small, but can be detected in the experimental results of the present study. Calculations show the increasing spinel liquidus due to Zn^{2+} in spinel solid solution. Spinel liquidus was not analyzed experimentally in the present study.

In addition to phase equilibria and distribution of elements, thermodynamic calculations provide information on the oxygen partial pressure in the system. Figure 4a shows $P(O_2)$ in the experiments calculated for the measured slag compositions. Distribution coefficients plotted as a function of $P(O_2)$ are shown in Fig. 4b. The experimental measurements by Moon et al. [12] are plotted as well for comparison. According to Yazawa [55], the slope of the curve log$_{10}$L vs Log[$P(O_2)$] must be constant and indicates the oxidation state of the minor element in slag. The slope should be the highest for Bi, reflecting a higher oxidation state in the slag. In the case of PbO–FeO–Fe$_2$O$_3$–SiO$_2$ slag in equilibrium with Pb metal, there will be a significant deviation from this rule, because with increasing $P(O_2)$, more and more PbO dissolves in the slag. The molar ratio Si/(Pb + Fe) in the slag equilibrated with tridymite increases, as can be seen in Fig. 3a. The structure of the slag changes, affecting the activity coefficients of oxides of minor elements in the slag. In the model for slag, strong positive interaction parameters are assigned for Ag$_2$O–SiO$_2$, Au$_2$O–SiO$_2$, and Bi$_2$O$_3$–SiO$_2$
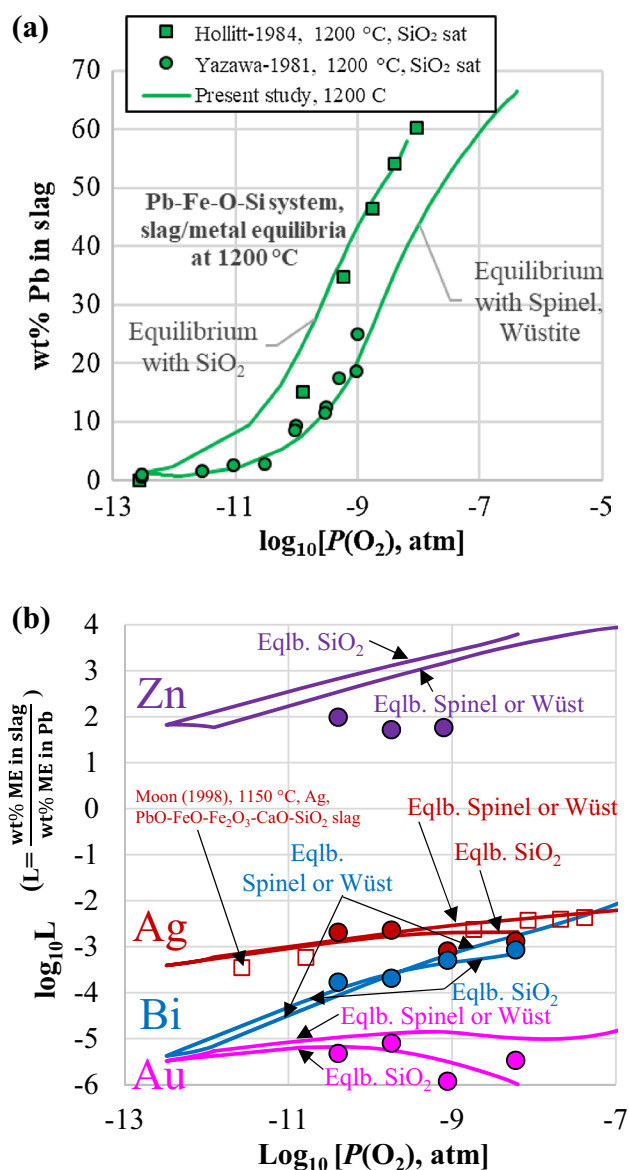

Fig. 4 **a** Relationship between $P(O_2)$ and wt% Pb in slag for slag/Pb equilibria in the Pb–Fe–O–Si system. Symbols are literature data [56, 57]. **b** Distribution coefficients of Ag, Au, Bi, and Zn between slag and liquid Pb as a function of $P(O_2)$. Circles are experimental results of the present study, empty squares are from Moon [12]. Lines are thermodynamic calculations of the present study (Color figure online)

pairs, but negative interaction parameters for ZnO–SiO$_2$. This is why in Fig. 4b, the calculated distribution coefficients for slags in equilibrium with SiO$_2$ demonstrate decreasing slope at higher $P(O_2)$ for Ag, Au, and Bi. This effect is detected in the experiment. Initial model predictions for Bi were close to the experimental results, but somewhat higher. Since no data are available in the literature for PbO–Bi$_2$O$_3$–SiO$_2$ phase diagram, one model parameter $g^{001}_{PbSi(Bi)}$ = +8368 J mol^{-1} was introduced and

optimized to provide a better agreement with observed distribution coefficient.

For Zn, the discrepancies were found between experimental data and model predictions. The calculated slope for Zn is almost constant, which is not observed in the experiment. The disagreement can be attributed to the lower accuracy of measurement for very small concentrations in metal phase, close to the detection limit. The presence of the second phase with much higher concentration may affect the results. Further studies are planned in PYROSEARCH to resolve the uncertainty and establish the thermodynamic properties of Zn in slag, copper metal, lead metal, and mattes of various compositions. Higher concentrations of Zn in slag and lower $P(O_2)$ can be used to achieve the concentration in metal at least 0.2 wt% Zn.

Conclusions

Distributions of minor concentrations of Ag, Au, Bi, and Zn between liquid slag and liquid Pb metal phase in the Pb–Fe–O–Si system have been determined experimentally using the equilibration/quenching/EPMA or LA-ICP-MS technique. The experimentally obtained distribution coefficients slag/metal follow the sequence $Zn \gg Ag > Bi \gg Au$. Experimental results were compared with thermodynamic calculations, performed using FactSage software and a custom thermodynamic database. The database was built using several types of literature data: calorimetric, phase equilibria, activity, and distribution data. Good agreement between the thermodynamic calculations and experimental results was obtained for Bi, Ag, and Au. The effect of oxygen partial pressure on the distribution coefficients was established. For Zn, the agreement is qualitative. In the experiment, the equilibrium concentration of Zn in the lead metal phase was too low for quantitative analysis.

Compliance with Ethical Standards

Conflict of interest On behalf of all authors, the corresponding author states that there is no conflict of interest.

References

1. Khaliq A, Rhamdhani MA, Brooks G, Masood S (2014) Metal extraction processes for electronic waste and existing industrial routes: a review Australian perspective. Resources 3:152–179. https://doi.org/10.3390/resources3010152
2. Tesfaye F, Lindberg D, Hamuyuni J, Taskinen P, Hupa L (2017) Improving urban mining practices for optimal recovery of resources from e-waste. Miner Eng 111:209–221. https://doi.org/10.1016/j.mineng.2017.06.018
3. Shishin D, Hayes PC, Jak E (2018) Multicomponent thermodynamic databases for complex non-ferrous pyrometallurgical processes. In: Davis B, Moats M, Wang S (eds) Extraction 2018: Proceedings of the first global conference on extractive metallurgy. Springer, New York, pp 853-868. https://doi.org/10.1007/978-3-319-95022-8_68
4. Jak E (2018) Modelling metallurgical furnaces—making the most of modern research and development techniques. In: Davis B, Moats M, Wang S (eds) Extraction 2018: Proceedings of the first global conference on extractive metallurgy. Springer, New York, pp 103-125. https://doi.org/10.1007/978-3-319-95022-8_8
5. Shishin D, Hidayat T, Chen J, Hayes PC, Jak E (2019) Combined experimental and thermodynamic modeling investigation of the distribution of antimony and tin between phases in the Cu-Fe-O-S-Si system. Calphad 65:16–24
6. Shishin D, Hidayat T, Chen J, Hayes PC, Jak E (2018) Integrated experimental study and thermodynamic modelling of the distribution of arsenic between phases in the Cu-Fe-O-S-Si system. J Chem Thermodyn 135:175–182
7. Shishin D, Hidayat T, Chen J, Hayes PC, Jak E (2018) Experimental Investigation and thermodynamic modelling of the distributions of Ag and Au between slag, matte and metal in the Cu-Fe-O-S-Si system. J Sustain Metal 5:240–249. https://doi.org/10.1007/s40831-019-00218-w
8. Shevchenko M, Jak E (2019) Experimental liquidus studies of the Pb-Fe-Si-O system in air. J Phase Equilib Differ 40:319–355. https://doi.org/10.1007/s11669-019-00727-x
9. Shevchenko M, Jak E (2018) Experimental liquidus studies of the Pb-Fe-Si-O system in equilibrium with metallic Pb. Metall Mater Trans B 49:159–180. https://doi.org/10.1007/s11663-017-1136-0
10. Shevchenko M, Jak E (2019) Thermodynamic optimization of the PbO-FeO-Fe$_2$O$_3$-SiO$_2$ system. Calphad. https://doi.org/10.1016/j.calphad.2019.101670
11. Moon N, Hino M, Lee Y, Itagaki K (1999) Composition region of homogeneous liquid phase in lead-containing slas related to QSL process. Metal Rev MMIJ 16:3–14
12. Moon N, Hino M, Lee Y, Itagaki K (1998) Phase equilibrium and minor elements distribution between metallic lead and PbO-FeO$_x$-CaO-SiO$_2$ or PbO-FeO$_x$-CaO-SiO$_2$-ZnO Slag at 1423K. Metal Rev MMIJ 15:38–62
13. Jak E (2012) Integrated experimental and thermodynamic modelling research methodology for metallurgical slags with examples in the copper production field. In: Proceedings of Paper presented at the 9th International Conference on Molten Slags, Fluxes and Salts (MOLTEN12), Beijing, China,
14. Jak E, Hayes PC, Lee H-G (1995) Improved methodologies for the determination of high temperature phase equilibria Korean. J Miner Mater Inst (Seoul) 1:1–8
15. Shevchenko M, Jak E (2019) Experimental liquidus study of the binary PbO-ZnO and ternary PbO-ZnO-SiO$_2$ systems. Ceram Int 45:6795–6803. https://doi.org/10.1016/j.ceramint.2018.12.172
16. Bale CW et al (2016) FactSage thermochemical software and databases, 2010–2016. CALPHAD 54:35–53. https://doi.org/10.1016/j.calphad.2016.05.002

17. Fallah-Mehrjardi A, Hidayat T, Hayes PC, Jak E (2017) Experimental Investigation of gas/slag/matte/tridymite equilibria in the Cu-Fe-O-S-Si system in controlled gas atmospheres: development of technique. Metall Mater Trans B 48:3002–3016. https://doi.org/10.1007/s11663-017-1073-y

18. Chen J, Allen CM, Azekenov T, Ushkov LA, Hayes P, Jak E Quantitative determination of trace/ultra trace elements concentration in slag and matte generated in copper smelting using microanalysis techniques. In: Yamaguchi K (ed) Copper 2016, Kobe, Japan, 13-16 November 2016. MMIJ and JMIA, pp 1096-110

19. Pelton AD, Decterov SA, Eriksson G, Robelin C, Dessureault Y (2000) The Modified quasichemical model: I—binary solutions. Metall Mater Trans B 31:651–659

20. Pelton AD, Chartrand P (2001) The Modified Quasichemical Model: II–multicomponent solutions. Metall Mater Trans A 32:1355–1360

21. Hillert M (2001) The compound energy formalism. J Alloys Compd 320:161–176

22. Redlich O, Kister AT (1948) Thermodynamics of nonelectrolytic solutions: algebraic representation of thermodynamic properties and the classification of solutions. Ind Ing Chem 40:345–348

23. Eriksson G, Pelton AD (1993) Critical evaluation and optimization of the thermodynamic properties and phase diagrams of the $CaO-Al_2O_3$, $Al_2O_3-SiO_2$, and $CaO-Al_2O_3-SiO_2$ systems. Metall Trans 24:807–816

24. Hidayat T, Shishin D, Jak E, Decterov S (2015) Thermodynamic reevaluation of the Fe-O system. CALPHAD 48:131–144

25. Decterov SA, Jak E, Hayes PC, Pelton AD (2001) Experimental study and thermodynamic optimization of the Fe-Zn-O system. Metall Mater Trans B 32:643–657

26. Shishin D, Prostakova V, Jak E, Decterov S (2016) Critical assessment and thermodynamic modeling of the Al–Fe–O system. Metall Mater Trans B 47:397–424

27. Hidayat T, Shishin D, Decterov SA, Jak E (2017) Experimental study and thermodynamic re-evaluation of the $FeO-Fe_2O_3$-SiO_2 system. J Phase Equilib Diffus 38:477–492. https://doi.org/10.1007/s11669-017-0535-x

28. Shevchenko M, Jak E (2019) Thermodynamic optimization of the binary systems $PbO-SiO_2$, $ZnO-SiO_2$, $PbO-ZnO$, and ternary $PbO-ZnO-SiO_2$. Calphad 64:318–326. https://doi.org/10.1016/j.calphad.2019.01.011

29. Shevchenko M (2019) Integrated experimental and thermodynamic modelling research on the multicomponent Pb-Cu-Fe-Zn-Ca-Si-O system. PhD Thesis, School of Chemical Engineering, The University of Queensland

30. Lee B-Z, Oh C-S, Lee DN (1994) A thermodynamic evaluation of the Ag-Pb-Sb system. J Alloys Compd 215:293–301

31. Wang J, Liu HS, Jin ZP (2004) Thermodynamic assessment of the Au-Pb system. CALPHAD 28:91–95. https://doi.org/10.1016/j.calphad.2004.05.003

32. David N, Hertz J, Fiorani JM (2003) Thermodynamic assessment of the Pb-Zn system. Z Metallkd 94:8–11. https://doi.org/10.3139/146.030008

33. Gierlotka W, Tung Y-C (2017) A new thermodynamic description of the Bi-Pb-Sn system. J Phase Equilib Diffus 38:814–828. https://doi.org/10.1007/s11669-017-0572-5

34. Hidayat T, Chen J, Hayes PC, Jak E (2018) Distributions of Ag, Bi, and Sb as minor elements between iron-silicate slag and copper in equilibrium with tridymite in the Cu-Fe-O-Si system at T = 1250 & #xB0;C and 1300 & #xB0;C (1523 K and 1573 K). Metall Mater Trans B. https://doi.org/10.1007/s11663-018-1448-8

35. Nagamori M, Mackey PJ, Tarassoff P (1975) Distribution of arsenic, antimony, bismuth, selenium, and tellurium between molten copper and white. Metal Metall Trans B 6B:197–198

36. Chen C, Wright S (2016) Distribution of Bi between slags and liquid copper. Metall Mater Trans B. https://doi.org/10.1007/s11663-016-0610-4

37. Takeda Y, Ishiwata S, Yazawa A (1983) Distribution equilibriums of minor elements between liquid copper and calcium ferrite slag. Trans Jpn Inst Met 24:518–528

38. Jimbo I, Goto S, Ogawa O (1984) Equilibria between silica-saturated iron silicate slags and molten copper-arsenic, copper-antimony, and copper-bismuth alloys. Metall Trans B 15B:535–541. https://doi.org/10.1007/bf02657385

39. Assal J, Hallstedt B, Gauckler LJ (1997) Thermodynamic assessment of the silver-oxygen system. J Am Ceram Soc 80:3054–3060

40. Shevchenko M, Shishin D, Jak E (2019) Experimental study and thermodynamic modelling of the $Ag_2O-PbO-SiO_2$ slag in equilibrium with silver metal Internal report. The University of Queensland, Pyrometallurgy Innovation Centre

41. Borisov A, Palme H (1996) Experimental determination of the solubility of Au in silicate melts. Miner Petrol 56:297–312. https://doi.org/10.1007/bf01162608

42. Han YS, Swinbourne DR, Park JH (2015) Thermodynamics of gold dissolution behavior in $CaO-SiO_2-Al_2O_3-MgO$sat slag system. Metall Mater Trans B 46:2449–2457. https://doi.org/10.1007/s11663-015-0421-z

43. Swinbourne DR, Yan S, Salim S (2005) The solubility of gold in metallurgical slags. Trans Inst Min Metall C 114:C23–C29. https://doi.org/10.1179/037195505x28429

44. Avarmaa K, O'Brien H, Taskinen P (2016) Equilibria of gold and silver between molten coppe -$SiO_2-Al_2O_3$ slag in WEEE smelting at 1300 °C. In: Ramana G. Reddy PC, P. Chris Pistorius, and Uday Pal (eds) Advances in molten slags, fluxes, and salts: proceedings of The 10th international conference on molten slags, fluxes and salts (MOLTEN16). The Minerals, Metals & Materials Society, pp 193-202

45. Sukhomlinov D, Taskinen P (2017) Distribution of Ni, Co, Ag, Au, Pt, Pd between copper metal and silica saturated iron silicate slag. In: Proceedings of EMC 2017, Leipzig, Germany, pp 1-10

46. Jak E, Decterov SA, Wu P, Hayes PC, Pelton AD (1997) Thermodynamic optimisation of the systems $PbO-SiO_2$, $PbO-ZnO$, $ZnO-SiO_2$ and $PbO-ZnO-SiO_2$. Metall Mater Trans B 28B:1011–1018

47. Shevchenko M, Jak E (2019) Experimental Liquidus Studies of the Zn-Fe-Si-O System in air. IJMR 110:600–607. https://doi.org/10.3139/146.111779

48. Hidayat T, Hayes PC, Jak E (2018) Phase equilibria in the ZnO-"FeO"-SiO_2 system in reducing atmosphere and in the ZnO-"FeO"-SiO_2-"Cu_2O" system in Equilibrium with liquid copper metal at 1250°C (1523 K). Metall Mater Trans B 49:1766–1780. https://doi.org/10.1007/s11663-018-1285-9

49. Risold D, Hallstedt B, Gauckler LJ, Lukas HL, Fries SG (1995) The bimuth-oxygen system. J Phase Equilib 16:223–234. https://doi.org/10.1007/bf02667306

50. Diop I, David N, Fiorani JM, Podor R, Vilasi M (2009) Experimental investigations and thermodynamic description of the $PbO-Bi_2O_3$ system. J Chem Thermodyn 41:420–432. https://doi.org/10.1016/j.jct.2008.10.012

51. Onderka B, Fitzner K, Kopyto M, Przybyło W (2017) Thermodynamics of $Bi_2O_3-SiO_2$ system. J Mining Metal B 53:223–231

52. Lu J, Qiao LJ, Fu PZ, Wu YC (2011) Phase equilibrium of $Bi_2O_3-Fe_2O_3$ pseudo-binary system and growth of $BiFeO_3$ single crystal. J Cryst Growth 318:936–941. https://doi.org/10.1016/j.jcrysgro.2010.10.181

53. Maitre A, Francois M, Gachon JC (2004) Experimental study of the $Bi_2O_3-Fe_2O_3$ pseudo-binary system. J Phase Equilib Diffus 25:59–67. https://doi.org/10.1007/s11669-004-0171-0

54. Phapale S, Mishra R, Das D (2008) Standard enthalpy of formation and heat capacity of compounds in the pseudo-binary

Bi_2O_3-Fe_2O_3 system. J Nucl Mater 373:137–141. https://doi.org/10.1016/j.jnucmat.2007.05.036

55. Yazawa A, Nakazawa S, Takeda Y Distribution behavior of various elements in copper smelting systems. In: Proceedings of International Sulfide Smelting Symposium, San Francisco, USA, 1983. Metall. Soc. AIME, pp 99-117

56. Hollitt MJ, Willis GM, Floyd JM (1984) Thermodynamics of the silica-saturated Pb-Fe-O-SiO_2 system at 1200°C. 2nd Int Symp Metal Slags Fluxes. 10.1016/j.calphad.2019.01.011

57. Yazawa A, Takeda Y, Waseda Y (1981) Thermodynamic properties and structure of ferrite slags and their process implications. Can Metall Q 20:129–134